

Exoplanet Predictions Based on Harmonic Orbit Resonances

Markus J. Aschwanden¹

¹) *Lockheed Martin, Solar and Astrophysics Laboratory, Org. A021S, Bldg. 252, 3251 Hanover St., Palo Alto, CA 94304, USA; e-mail: aschwanden@lmsal.com*

and

Felix Scholkmann²

²) *Research Office for Complex Physical and Biological Systems, Mutschellenstr. 179, 8038 Zürich, Switzerland; e-mail: felix.scholkmann@gmail.com*

ABSTRACT

The current exoplanet database includes 5454 confirmed planets and candidate planets observed with the KEPLER mission. We find 932 planet pairs from which we extract distance and orbital period ratios. While earlier studies used the Titius-Bode law or a generalized version with logarithmic spacing, which both lack a physical model, we employ here the theory of harmonic orbit resonances, which contains quantized ratios instead, to explain the observed planet distance ratios and to predict undetected exoplanets. We find that the most prevailing harmonic ratios are (2:1), (3:2), and (5:3), in 73% of the cases, while alternative harmonic ratios of (5:4), (4:3), (5:2), (3:1) occur in 27% of the other cases. Our orbital predictions includes 171 exoplanets, 2 Jupiter moons, one Saturn moon, 3 Uranus moons, and 4 Neptune moons. The accuracy of the predicted planet distances amounts to a few percent, which fits the data significantly better than the Titius-Bode law or a logarithmic spacing. This information may be useful for targeted exoplanet searches with Kepler data and to estimate the number of live-carrying planets in habitable zones.

Subject headings: planetary systems — planets and satellites: general — stars: individual

1. INTRODUCTION

The recent discoveries of exoplanets has currently amassed a catalog of over 5000 exoplanets (Han et al. 2014), which contains the names of the host stars, the semi-major axes, and orbital periods of the associated exoplanets (see website: *exoplanets.org*). The unprecedented statistics of these orbital parameters allows us for the first time to determine whether the planets are distributed in random distances from the central star, or in some systematic order, as it is expected from physical models of harmonic resonance orbits (Peale 1976). Data analysis of statistical exoplanet databases therefore provides key information on the physical process of the formation of planetary systems, as well as on the number and statistical probability of planets that are located in habitable zones around stars.

Orbital resonances in the solar system have been known for a long time (e.g., see review by Peale 1976). A particular clean example is given by the three Galilean satellites of Jupiter (Io, Europa, Ganymede), for which Laplace (1829) demonstrated their long-term stability based on celestial mechanics perturbation theory. Other examples are the gaps in the rings of Saturn, the resonances of asteroids with Jupiter (Trojans, Thule,

Hilda, Griqua, Kirkwood gaps), as well as the harmonic orbital periods of the planets in our solar system. Low harmonic (integer) numbers of orbital periods warrant frequent conjunction times, which translates into frequent gravitational interactions that can stabilize a three-body system of planets (or asteroids). The stability of orbital resonances has been explained in terms of the libration of coupled pendulum systems (Brown and Shook 1933). Physical descriptions of celestial resonance phenomena are reviewed in Peale (1976).

Empirical models of planet distances, such as the Titius-Bode law, or the generalized Titius-Bode law, are not consistent with harmonic orbit ratios, and lack a physical model. It is therefore imperative not to use such empirical laws for the prediction of exoplanets, but rather physical models based on harmonic orbital resonances, which we pursue in this study. Previous predictions of (missing) exoplanets are based on the original Titius-Bode law (Cuntz 2012; Poveda and Lara 2008; Qian et al. 2011), the logarithmic spacing of the generalized Titius-Bode law (Bovaird and Lineweaver 2013; Bovaird et al. 2015; Huang and Bakos 2014), an exponential function (Lovis et al. 2011), or a multi-modal probability distribution function (Scholkmann 2013). A recent study analyzed the statistical distribution of mean motion resonances and near-resonances in 1176 exoplanet systems, finding a preference for (3:2) and (2:1) resonances in the overall, but large variations of the harmonic ratio for different planet types, grouped by their semi-major axis size, their mass, or host star type (Ghilea 2015).

In this study we identify a complete set of principal harmonic numbers that explain all observed exoplanet distances and infer the statistical probability of the harmonic number ratios found in exoplanets. Based on this analysis we present predictions of so far un-detected exoplanets in 190 exoplanet systems. We describe the data analysis method and the observational results in Section 2, followed by a discussion conclusions in Section 3.

2. OBSERVATIONS AND DATA ANALYSIS METHOD

2.1. Data Set Statistics

We access the web-based exoplanet database <http://exoplanets.org> and find at the time of this analysis (2017 May 10) a total of 5454 detected exoplanets, which includes confirmed planets as well as candidate planets from the *Kepler* mission. Most of the exoplanets represent single detections in a star system, which is the case in 3860 cases. Double planet detections occur in 472 star systems, triple-planet systems in 128, quadruple-planet systems in 44, quintuple-planet systems in 14, and sextuple-planet systems in 2 star systems. The largest planet systems have 7 detections of planets, such as the KIC-11442793 and the TRAPPIST-1 system (Gillon et al. 2017). We updated the TRAPPIST-1 system, with 3 stars given in the exoplanet data base, to 7 stars given in Gillon et al. (2017), analyzed also by Pletser and Basano (2017) and Scholkmann (2017). All these exoplanet detections are associated with a total of 4522 different stars (Table 1).

For our analysis we are most interested in studying harmonic resonance orbit ratios, which requires at least 2 neighbored exoplanets per star, which amounts to a total of 622 exoplanets, or a number of 932 planet pairs. We attempt also predictions of missing planets, which requires at least 3 planets per star, which is feasible in 190 exoplanet systems.

2.2. Orbital Period Ratio Distribution

An important result of our analysis is the distribution of orbital period ratios $Q_i = P_{i+1}/P_i$, where P_i and P_{i+1} , $i = 1, \dots, n_p - 1$ are the orbital time periods in a planetary system with n_p planets. These orbital periods P_i are directly related to the semi-major axis of the planets (i.e., their mean distance D to the center of the host star), according to Kepler’s 3^{rd} law,

$$D = P^{2/3} . \quad (1)$$

We plot a histogram of orbital period ratios Q_i for all $N = 932$ planet pairs in Fig. 1 (top panel), sampled in a range of $P = [0.5, 3.5]$ with a histogram bin width of $dP = 0.04$. These period ratios are defined from the ratios of the outer planet distance P_{i+1} to the inner planet distance P_i , which is always larger than unity by definition, i.e., $P_i > 1$, since the inner planets rotate faster around the Sun than the outer planets. We are adding error bars $\sigma_N(P_i) \propto \sqrt{N_i}$ in Fig. 1 (top panel) as expected from Poisson statistics.

What is striking about the period distribution $N(P)$ shown in Fig. 1 (top panel) is that the periods do not follow a smooth (approximately log-normal) distribution, but rather exhibit significant peaks at the harmonic values of $Q = (3 : 2) = 1.5$ and at $P = (2 : 1) = 2.0$, which involve the lowest possible harmonic numbers 1, 2, and 3. In a previous study on our own solar system and the moons around planets we noticed a dominance of five low harmonic ratios, i.e., (3:2), (5:3), (2:1), (5:2), and (3:1) (Aschwanden and McFadden 2017). Interestingly, we find now that exoplanets confirm the preponderance of harmonic ratios (3:2) and (2:1), while the other ratios (5:3), (3:1), and (5:2) are less significant.

The distribution of harmonic ratios drops steeply from $Q = 1.5$ towards a value of $Q > 1.0$ at the low side, while the upper end extends all the way to $Q \approx 1229$. The extended tail at the upper end can be explained by a large number of missing (undetected) planets, where the most extreme ratio applies to the case where the innermost and the outermost planet is detected only. For our solar system, this maximum ratio would be the orbital period ratio between Mercury and Pluto, i.e., $Q_{max} = 248 \text{ yrs} / 0.24 \text{ yrs} \approx 1033$.

2.3. Orbital Period Ratios of Large Planet Systems

In Fig. 2 we show the orbital distances D for the 18 largest exoplanet systems (in alphabetical order), which includes all cases with 5, 6, or 7 planets per star. Each panel in Fig. 2 displays the predicted planet distance (from the central star) to the observed planet distance. While we quote harmonic ratios of the orbital periods throughout the paper, the corresponding distances (as shown in Fig. 2) are simply calculated from Kepler’s 3^{rd} law (Eq. 1). If we limit ourselves to a maximum orbit ratio of $Q \leq 3.0$, we find that all observed orbital period ratios in this subset (shown in Fig. 2) can be explained by 7 small harmonic ratios in the range of (5:4)=1.25, (4:3)=1.333, (3:2)=1.5, (5:3)=1.667, (2:1)=2.0, (5:2)=2.5, (3:1)=3.0, which we define as “principal harmonic ratios”. From these largest 18 systems shown in Fig. 2 we find that half of them are “gap-free exoplanet systems”, which means that all detected period ratios Q_i can be explained with these principal harmonic ratios in the range of $1.25 \leq Q \leq 3.0$, such as Kepler-11, Kepler-154, Kepler-292, Kepler-33, Kepler-444, Kepler-55, Kepler-80, Kepler-84, and TRAPPIST-1. In all other cases we find some “gaps”, which are manifested by orbital period ratios of $Q > 3.0$. These gaps are likely to be produced by missing (undetected) planets (marked with red diamonds in Fig. 2, such as 55-Cnc, HD-10180, KIC-11442793, Kepler-169, Kepler-186, Kepler-20, Kepler-32, and Kepler-62. Since the largest exoplanet systems have 7 members so far, while our own solar system hosts 10 planets, it is likely that there are more missing exoplanets outside the so far detected gap-free sequences.

2.4. Strategy for Predicting Missing Exoplanets

Previous studies developed strategies to predict missing (undetected) exoplanets from the generalized Titius-Bode law, which assumes a constant geometric progression factor Q , i.e., $T_{i+1}/T_i = Q$, (e.g., Bovaird and Lineweaver 2013). In a recent study, however, we found that the observational data support quantized harmonic resonance ratios, such as $Q = 1.5, 1.667, 2.0, 2.5, 3.0$ (Aschwanden and McFadden 2017), rather than a constant progression factor Q . Such a quantization thus has to be included in a search strategy of missing (undetected) exoplanets. On the other side, the generalized Titius-Bode law is simpler to fit to data, because it is controlled by a single free parameter Q , while fitting a harmonic resonance model is more ambiguous due to a larger number of quantized parameters Q_i .

The problem can be formulated as an optimization problem of predicting a gap-free sequence of harmonic ratios,

$$P_{i+1}^{pred} = P_i^{pred} \times Q_i, \quad i = 1, \dots, n_p - 1, \quad (2)$$

where the n_p orbital period ratios Q_i are drawn from the range of principal harmonic ratios in such a way that the observed subset of $n_{det} \leq n_p$ orbital periods P_i^{obs} of the detected exoplanets matches the predicted periods P_i^{pred} .

In the following we develop a search strategy that is consistent with harmonic resonance orbits and consists of the following steps: (1) We define a range of 7 *principal low harmonics*: (5:4)=1.25, (4:3)=1.333, (3:2)=1.5, (5:3)=1.667, (2:1)=2.0, (5:2)=2.5, (3:1)=3.0. Neighbored exoplanet orbit pairs with ratios in the range of $1.1 \lesssim Q_i \lesssim 3.1$ are attributed to the closest principal harmonic ratio. (2) Orbital ratios in the range of $1.0 \leq Q_i \lesssim 1.1$ are interpreted as planet pairs in identical harmonic resonance zones, which are found only for very small bodies (like asteroids or moons of Jupiter and Saturn with diameters of $d < 500$ km); (3) Detected planet pairs with orbital periods of $Q \gtrsim 3.1$ are interpreted as gaps with one or more missing (undetected) planets. Since a gap Q_{obs} has to be filled by n_{miss} planets, i.e., $Q_{obs} \approx (Q_{gap})^{(n_{miss})}$, we determine the number n_{miss} of missing planets from the observed interval $Q_{obs} = T_{i+1}/T_i$ by

$$n_{miss} = Round \left[\frac{\log Q_{obs}}{\log Q_{gap}} \right], \quad (3)$$

where *Round* represents a rounding function to the next integer number. The characteristic ratio Q_{gap} is estimated from the best-fitting value of the 5 most frequent principal harmonic ratios, i.e., $Q_{gap} = 1.5, 1.667, 2.0, 2.5, \text{ and } 3.0$. The best-fitting value Q_{gap} is simply determined by minimizing the mean deviation σ_P between the observed (P_i^{obs}) and the predicted orbital periods (P_i^{pred}),

$$\sigma_P = \frac{1}{n_{obs}} \sum_{i=0}^{n_{obs}} \frac{|P_i^{pred} - P_i^{obs}|}{P_i^{obs}}, \quad (4)$$

which translates into a mean deviation σ_D of planet distances D according to Kepler's law (Eq. 1),

$$\sigma_D = \frac{1}{n_{obs}} \sum_{i=0}^{n_{obs}} \frac{|D_i^{pred} - D_i^{obs}|}{D_i^{obs}}, = \sigma_P^{2/3}. \quad (5)$$

An additional constraint is the estimated maximum number of planets per system, which we choose to be $n_{p,max} = 11$, based on the number of planets detected in our solar system ($n_p = 10$ including the asteroids), and the number of Jupiter moons ($n_p = 9$) or Saturn moons ($n_p = 10$) that fit the scheme (see Appendix A for our solar system and planetary moon systems).

These best-fit mean deviations $D_{pred}/D_{obs} - 1 = \sigma_D$ are listed in the 18 panels in Fig. 2. We see that these best-fit solutions of harmonic ratios match the observed orbital period ratios typically within accuracy of $\approx 1\% - 5\%$. The most accurate harmonic ratios with an accuracy of $\approx 1\%$ are found for the planetary systems of Kepler-169, Kepler-32, Kepler-444, and TRAPPIST-1.

Of course, the estimated missing planets bear some ambiguity because the ratios in subsequent intervals in a gap can be permuted arbitrarily. For instance, if we take out a planet between two resonance zones of $Q_{i+1} = (3 : 2)$ and $Q_i = (2 : 0)$, the permuted sequence $Q_{i+1} = (2 : 0)$ and $Q_i = (3 : 2)$ yields an identical solution, and thus the predicted resonance at the location of the filled gap is only accurate to $(1.5 + 2.0)/2 = 1.75 \pm 0.25$, which is attributed to the closest admissible resonance ratio of $(5 : 3) = 1.667$ and yields a combined period ratio of $(5 : 3) \times (5 : 3) = 2.778$ in the gap, which is within 8% of the correct gap value $(3 : 2) \times (2 : 1) = 3.0$.

2.5. Statistical Probability of Quantized Periods

After we corrected each detected exoplanet sequence of orbital periods $Q_i, i = 1, \dots, n_p - 1$ per exoplanet system or star (for exoplanet systems with more than 3 detected exoplanets), by predicting missing exoplanet detections according to the algorithm described above, we can sample the distribution of predicted orbital periods, which is shown in Fig. 1 (bottom panel). The predicted distribution of orbital period ratios is now, as a consequence of the applied prediction scheme, quantized according to the 7 principal harmonic ratios, while no ratio is found outside the range of $1.25 \leq Q_i \leq 3.0$. What this quantized distribution reveals moreover, is the statistical probability for the individual harmonic ratios. According to the result shown in Fig. 1 (bottom panel), the highest probability is for the harmonic ratios of (3:2), (5:3), and (2:1), while the other four harmonic ratios are significantly rarer. The relative probabilities for each of the 7 principal harmonic ratios are (in order of decreasing probability): 26% for a ratio of (3:2), 25% for a ratio of (2:1), 22% for a ratio of (5:3), 14% for a ratio of (5:2), 6% for a ratio of (3:1), 4% for a ratio of (4:3), and 3% for a ratio of (5:4).

2.6. Catalog of Exoplanet Predictions

In Fig. 3 we list the planet distances of all 190 exoplanet systems with more than 3 planets. The observed period ratios amount of the 190 exoplanet systems amount to a total of $N_{det} = 128 \times 3 + 44 \times 4 + 14 \times 5 + 2 \times 6 + 2 \times 6 = 654$ values (see statistics in Table 1). The number of predicted exoplanets for this sample are marked with red numbers in Fig. 3, amounting to a total of 171 predictions. These predicted distances of undetected exoplanets can be used in targeted searches with Kepler data or others.

3. DISCUSSION AND CONCLUSIONS

The knowledge of planet distances from their host star provides us several important pieces of information. One central insight that can only be proven with reliable planet distance ratios is the physical formation process of planetary systems. A leading theory in this respect is the harmonic orbit resonance concept, which implies that multiple planets entrain into long-term stable orbits only once their orbits achieve a harmonic ratio with low numbers. Our analysis of 932 exoplanet pairs yielded evidence that the prevailing harmonic

ratios are (2:1), (3:2), and (5:3), which dominate in 73% of all exoplanet pairs, consistent with the finding of Ghilea (2015), while less additional harmonic ratios of (5:4), (4:3), (5:2), and (3:1) occur also, but are less frequent (in 27% of all cases). This relative probability of harmonic ratios in planet orbits is a quantitative result that can be tested with numerical simulations of n-body gravitational perturbation theory.

What is the predictive power of this exercise for missing exoplanets? Previous studies employed the generalized Titius-Bode law (e.g., Bouvaird and Lineweaver 2013), which assumes a constant geometric progression factor (or orbit period progression factor Q by applying Kepler’s 3rd law), also called logarithmic spacing. A constant progression factor has mostly been used for sake of mathematical simplicity, because it has only one free parameter, but it has no physical justification, and is actually inconsistent with harmonic orbital resonance theories, which predict quantized values of low harmonic number ratios, such as our set of 7 principal harmonic numbers. Therefore, the prediction of missing planets requires an algorithm that is based on low harmonic number ratios, which is more difficult to fit in the presence of gaps than a constant progression factor for logarithmic spacing. Consequently, in fitting a complete planet system without gaps (of missing undetected planets), each planet orbit period ratio has up to 7 free parameters (corresponding to the principal low harmonic ratios). Although this creates some ambiguity, since the best solution is insensitive to permutations of interpolated orbit period ratios, we eliminated this ambiguity by minimizing the difference between observed and modeled planet distances. In summary, the prediction of missing planets is based on solutions of orbital period sequences that contain only harmonic number ratios, rather than a constant logarithmic spacing.

The orbital predictions obtained in this study includes 2 Jupiter moons, one Saturn moon, 3 Uranus moons, 4 Neptune moons, and 171 exoplanets (Fig. 2 and Table in Fig. 3). The accuracy of the predicted planet distances amounts to a few percent. A previous study has shown that the harmonic orbit resonance model with quantized values fits the solar system and lunar systems better than the assumption of uniform logarithmic spacing (Aschwanden and McFadden 2017). This information may be useful for targeted searches of exoplanets with Kepler data, since it reduces the search parameter space. Moreover, it allows us to estimate the number of habitable planets in each exoplanet system (Chandler et al. 2016).

The existence of quantized values in planetary distances represents a system with (non-random) order, which falls into the category of self-organizing systems (Aschwanden and McFadden 2017). Self-organizing systems are characterized by regular geometric patterns that result from frequent local interactions in an initially disordered system (e.g., the libration of coupled pendulums). The principle of self-organization, however, should not be confused with the concept of *self-organized criticality* (Bak et al. 1987) in nonlinear dissipative systems, which is common in astrophysics also (Aschwanden et al. 2016).

APPENDIX A: Solar System and Planetary Moon Systems

As a consistency test we apply our prediction algorithm for missing exoplanets (Section 2.4) to our solar system and the moon systems described in a previous study (Aschwanden and McFadden 2017). The results are shown in Fig. 2c.

First we use the planet distances from Sun center for all 10 planets of our solare system, including the asteroid Ceres, shown in the panel labeled with Sun-10. Since no harmonic ratio larger than (3:1) occurs, our algorithm predicts no missing planet. In the second panel (labeled with Sun-9) we eliminate the asteroid Ceres, which is then detected as missing planet with our algorithm, because the harmonic ratio between Mars and Jupiter exhibits a ratio of ≈ 4.0 that is significantly larger than the largest admissible principal harmonic

ratio of 3.0. In the panel Sun-8 we eliminate Pluto in addition, which mimics the situation before 1930. In the panel Sun-7 we eliminate Neptune (before 1846), and in panel Sun-6 we eliminate Uranus (before 1781). In all four cases Sun-9, Sun-8, Sun-7, and Sun-6, our algorithm consistently flags only the asteroid Ceres, because in each situation the outermost planet is removed, while the remaining planets represents a gap-free sequence.

In panel Jupiter-7 (in Fig. 2c) we sample all Jupiter moons with a diameter of $d > 100$ km, namely Amalthea, Thebe, Io, Europa, Ganymede, Callisto and Himalia. Our algorithm predicts two missing moons between the two outermost detected moons Callisto and Himalia (similar to Fig. 6 in Aschwanden and McFadden 2017).

In panel Saturn-10 (in Fig. 2c) we sample all Saturn moons with a diameter of $d > 100$ km, namely Janus, Mimas, Enceladus, Thetis, Dione, Rhea, Tian, Hyperion, Japetus, and Phoebe. Our algorithm predicts one missing moon between the two outermost detected moons Japetus and Phoebe (similar to Fig. 7 in Aschwanden and McFadden 2017).

In panel Uranus-8 (in Fig. 2c) we sample all Uranus moons with a diameter of $d > 100$ km, namely Portia, Puck, Miranda, Ariel, Umbriel, Titania, Oberon, and Scycorax. Our algorithm predicts three missing moons between the two outermost detected moons Oberon and Scycorax (similar to Fig. 8 in Aschwanden and McFadden 2017).

In panel Neptune-6 (in Fig. 2c) we sample all Neptune moons with a diameter of $d > 100$ km, namely Galatea, Despina, Larissa, Proteus, Proteus, Triton, and Nereid. Our algorithm predicts three missing moons between the two outermost detected moons Triton and Nereid, and one missing moon between Proteus and Triton (similar to Fig. 9 in Aschwanden and McFadden 2017).

Altogether, our harmonic resonance model with an upper limit of $Q = 3.0$ for the highest admissible harmonic number predicts a total of 10 missing moons in our own planetary system. Note, that none of the predicted sequences exceeds a maximum of 11 moons per planetary system.

This research has made use of the Exoplanet Orbit Database and the Exoplanet Data Explorer at exoplanets.org. The first author acknowledges the hospitality and partial support for two workshops on “Self-Organized Criticality and Turbulence” at the *International Space Science Institute (ISSI)* at Bern, Switzerland, during October 15-19, 2012, and September 16-20, 2013, as well as constructive and stimulating discussions (in alphabetical order) with Sandra Chapman, Paul Charbonneau, Henrik Jeldtoft Jensen, Maya Paczuski, Jens Juul Rasmussen, John Rundle, Loukas Vlahos, and Nick Watkins. This work was partially supported by NASA contract NNX11A099G “Self-organized criticality in solar physics”.

REFERENCES

- Aschwanden, M.J., Crosby, N., Dimitropoulou, M., Georgoulis, M.K., Hergarten, S., McAteer, J., Milovanov, A., Mineshige, S., Morales, L., Nishizuka, N., Pruessner, G., Sanchez, R., Sharma, S., Strugarek, A., and Uritsky, V. 2016, *Space Science Reviews* 198, 47.
- Aschwanden, M.J. and McFadden, L.A. 2017, “Harmonic Resonances of Planet and Moon Orbits - From the Titius-Bode Law to Self-Organizing Systems”, URL=<http://www.lmsal.com/~aschwand/eprints/2017-planets.pdf>, arXiv:1701.08181 astro-ph.
- Bovaird, T. and Lineweaver, C.H., 2013, *MNRAS* 435, 1126.
- Bovaird, T., Lineweaver, C.H., and Jacobsen, S.K. 2015, *MNRAS* 448, 3608.
- Brown, E.W. and Shook, C.A. 1933, *Planetary Theory*, reprinted 1965. New York: Dover.
- Chandler, C.O., McDonald, I., and Kane, S.R. 2016, *ApJ* 151, 3.
- Cuntz, M. 2012, *PASJ* 64, 73.
- Ghilea, M.C. 2105, arXiv:1410.2478v3.
- Gillon, M., Triaud, A.H.M.J., Demory, B.O., et al. 2017, *Nature* 542, 456 (23 Feb 2017).
- Han, E., Wang, S., Wright, J.T., Feng, Y.K., Zhao, M., Fakhouri, O., Brown, J.I., and Hancock, C. 2014, *Pubs. Astron Soc. Pacific*, Vol. 126, Issue 943, pp. 827.
- Huang, C.X. and Bakos, G.A. 2014, *MNRAS* 442, 674.
- Lovis, C., Segransan, D., Mayor, M., Udry, S., Benz, W., Bertaux, J.L., Bouchy, F., Correia, A.C.M., et al. 2011, *A&A* 528, A112.
- Peale, S.J. 1976, *ARAA* 14, 215.
- Pletser, V. and Basano, L. 2017, arXiv preprint.
- Poveda, A. and Lara, P. 2008, *Revista Mexicana de Astronomia y Astrofísica* 44, 243.
- Qian, S.B., Liu, L., Liao, W.P., Li, J., Zhu, L.Y., Dai, Z.B., He J.J., Zhao, E.G., Zhang, J., and Li, K. 2011, *MNRAS* 414, L16.
- Scholkmann, F. 2013, *Progress in Physics* Vol. 9 (4), 85.
- Scholkmann, F. 2017, *Progress in Physics* Vol. 13, 125.

Table 1. Statistics of analyzed data set, using the Exoplanet Orbit Database (EOD) at exoplanets.org, (status of 2017 May 10).

Data set	Number
Number of detected exoplanets	5454
Number of exoplanet associated stars	4522
Number of stars with 1 exoplanet	3860
Number of stars with 2 exoplanets	472
Number of stars with 3 exoplanets	128
Number of stars with 4 exoplanets	44
Number of stars with 5 exoplanets	14
Number of stars with 6 exoplanets	2
Number of stars with 7 exoplanets	2
Number of planet-pair orbit ratios	932

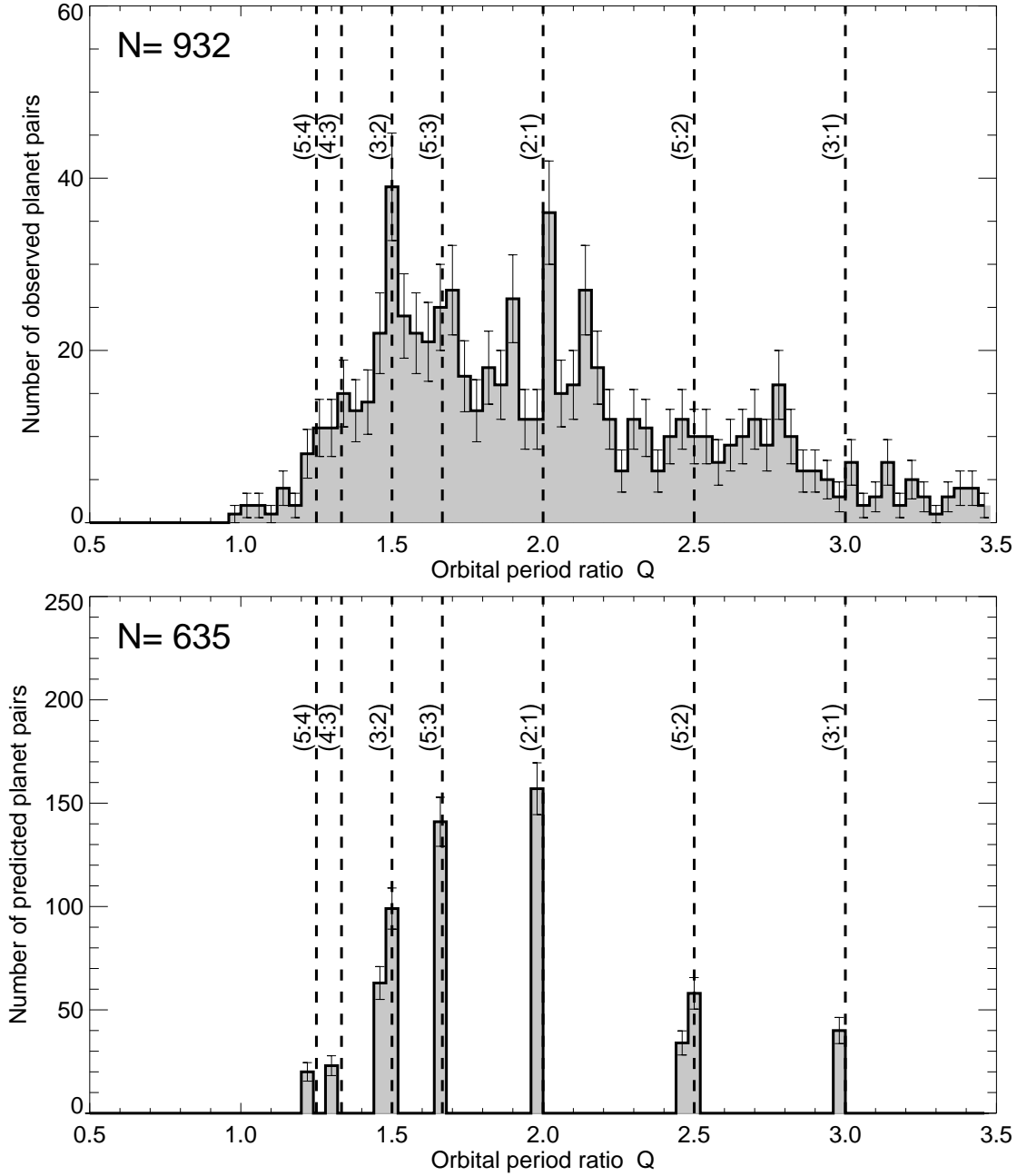


Fig. 1.— *Top*: The distribution of orbital period ratios Q in all 932 cases of planet pairs measured in the exoplanet database, using the version of 2017-May-10, which contains confirmed planets as well as candidate planets from the Kepler mission. The error bars conform to Poisson statistics. The 7 principal harmonic ratios are marked with vertical dashed lines. *Bottom*: The predicted quantized distribution of orbital period ratios Q in complete (gap-free) sequences of exoplanet detections (with at least 3 detections), obtained after filling gaps with $Q > 3.0$ with a search strategy described in Section 2.4.

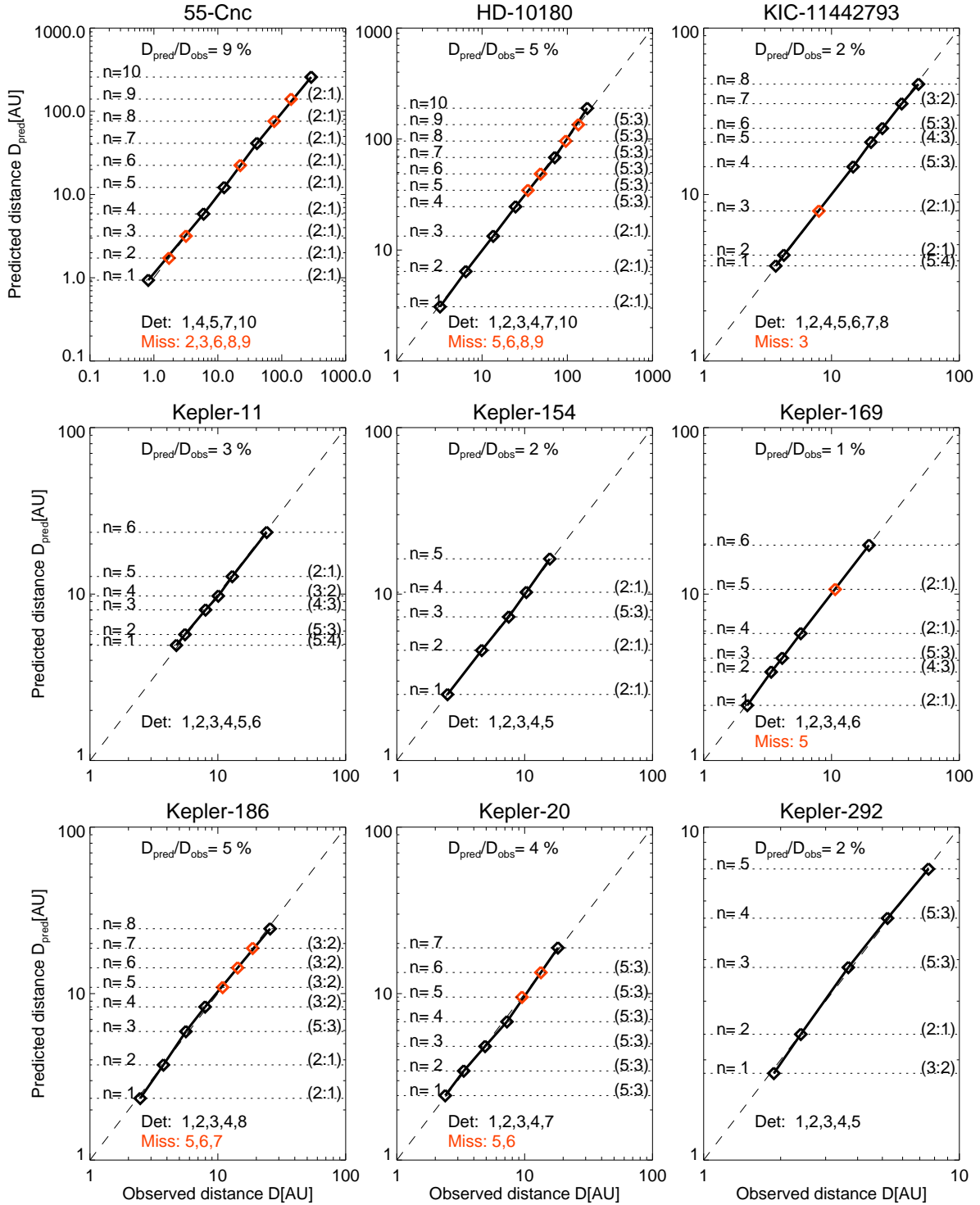
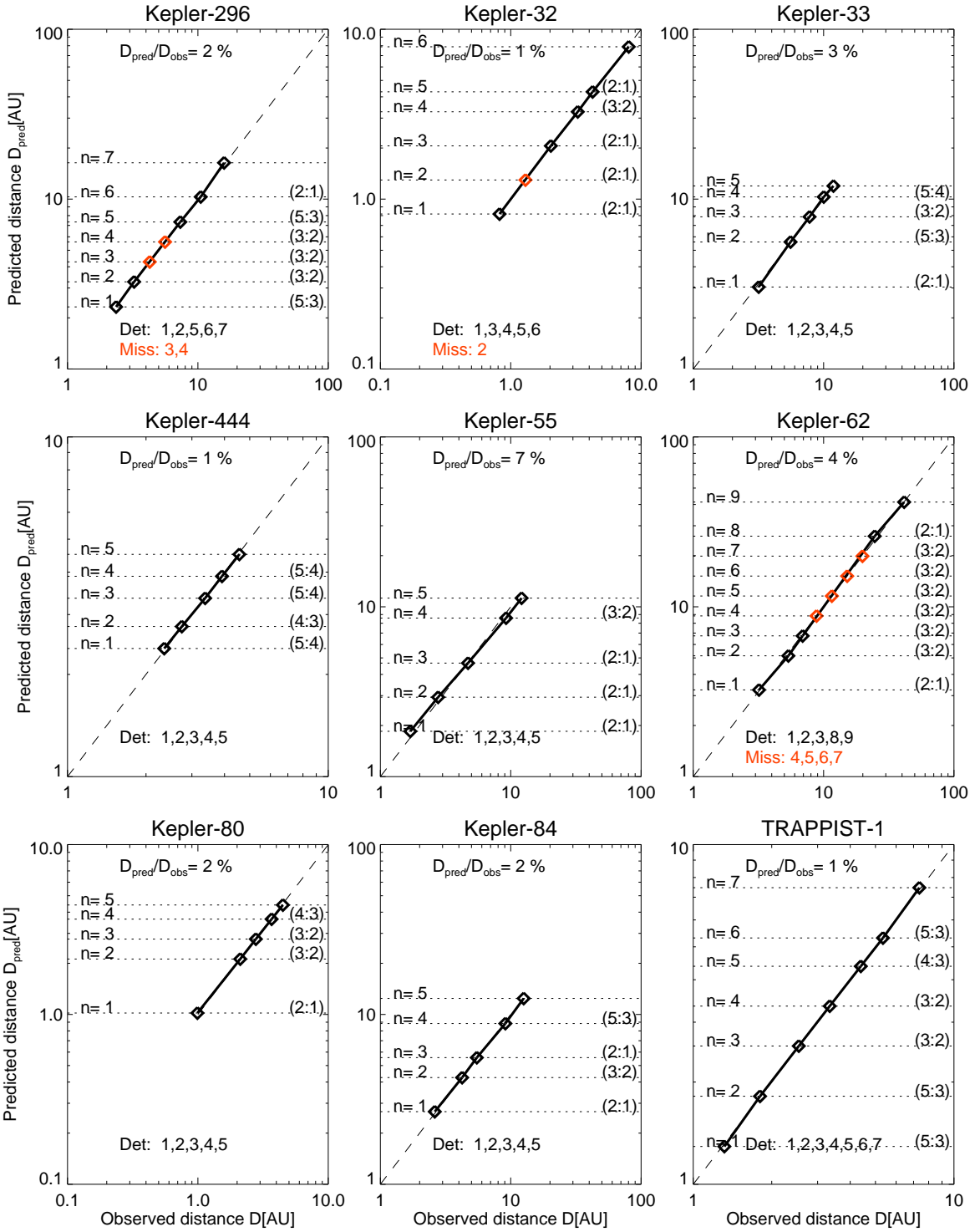


Fig. 2.— The predicted distances D^{pred} versus the observed distances D^{obs} of exoplanets from their central star in large exoplanet systems (with 5, 6, or 7 members). The detected exoplanets are marked with black diamonds, and the predicted exoplanets with red diamonds. The numeration corresponds to the complete systems that includes the predicted exoplanets. The average deviation between the predicted and observed distances, D_{pred}/D_{obs} , are given in percentages, the best-fit harmonic ratios are given on the right side, and the numeration of the detected and missing planets (red) are indicated near the bottom of each panel.



Star	Planet distances [AU]									
55-Cnc	0.94	1.72	3.18	5.85	12.17	22.42	41.29	76.07	140.11	258.09
61-Vir	2.66	5.52	11.49	23.90						
GJ-163	4.28	8.89	12.50	17.58	24.71	34.73	48.82	68.63		
GJ-581	2.15	3.02	5.57							
GJ-876	1.56	2.88	5.30	9.76	15.49	24.59				
HD-10180	3.08	6.41	13.34	24.58	34.55	48.57	68.27	95.97	134.91	189.65
HD-181433	4.44	8.18	15.07	27.76	51.13		94.19	173.49		
HD-20794	7.06	11.21	20.66							
HD-37124	28.00	51.58	95.01	150.82						
HD-40307	2.82	4.47	7.10							
HD-69830	4.17	5.47	7.16	9.39	12.30	16.12	21.12	27.68	36.27	
HD-7924	2.97	6.18	8.69							
HIP-14810	3.89	6.17	9.79	15.55	24.68	39.17	62.18	98.71		
HIP-57274	3.80	5.34	7.51	10.55	14.84	20.86	29.32	41.21	57.93	
HR-8799	646.14	1190.20	1889.33	2999.12						
K2-3	4.70	8.66	12.17							
KIC-11442793	3.73	4.33	7.97	14.68	20.63	25.00	35.14	46.04		
KOI-1082.	2.50	3.51	4.60							
KOI-1358.	1.83	2.39	3.13	4.11						
KOI-1475.	1.36	2.83	4.50							
KOI-1563.	2.20	3.10	4.06							
KOI-1576.	4.85	5.63	7.91							
KOI-1590.	1.81	2.87	5.29							
KOI-1681.	1.61	2.26	3.58	4.69	6.15	8.06				
KOI-1860.	2.13	3.37	5.36	8.50						
KOI-2037.	3.13	4.11	8.54	17.77						
KOI-2093.	1.02	1.87	3.45							
KOI-2169.	1.68	2.20	2.66							
KOI-2174.	3.48	4.04	6.41	10.18						
KOI-2248.	1.83	2.12	4.41							
KOI-2433.	3.34	4.69	6.60	9.27	14.72	19.29				
KOI-2579.	1.92	2.33	4.84							
KOI-279.	3.81	6.05	9.60							
KOI-285.	5.56	8.83	14.02							
KOI-2859.	2.03	2.66	3.08							
KOI-3083.	3.37	4.08	4.74							
KOI-3425.	2.14	3.95	7.27							
KOI-3444.	2.03	3.23	5.13	5.95	9.44	14.99				
KOI-353.	5.18	9.55	12.51	16.39	21.48	28.15				
KOI-4524.	2.28	2.76	3.88							
KOI-6242.	16.81	19.51	35.93							
KOI-85.	1.75	3.22	3.90							
KOI-94.	2.37	4.92	7.81	14.39						
KOI-945.	8.90	11.67	16.40							
Kepler-102	3.05	4.84	6.34	8.92						
Kepler-106	3.47	5.51	7.23	9.47	12.41					
Kepler-107	2.14	2.81	3.95	6.27						
Kepler-11	4.93	5.72	8.04	9.73	12.76	23.50				
Kepler-122	3.41	5.42	7.62	10.71						
Kepler-124	2.34	3.71	5.88	9.34						
Kepler-1254	2.32	3.27	4.59							
Kepler-126	4.87	7.73	10.87	15.28	21.48					
Kepler-127	5.97	9.47	13.31							
Kepler-132	3.09	3.59	7.46	9.78	12.81	16.79	22.00			
Kepler-1388	3.36	5.33	7.50	10.54						
Kepler-142	1.55	2.85	5.93	12.34						
Kepler-148	1.41	2.59	3.65	5.12	7.20	10.13	14.23			
Kepler-149	9.18	14.57	30.31							
Kepler-150	2.37	3.76	5.28	9.73						
Kepler-154	2.49	4.59	7.29	10.25	16.28					
Kepler-1542	2.06	2.49	2.89	3.35						
Kepler-157	1.44	2.29	3.63	5.76						
Kepler-164	3.09	4.90	9.02							
Kepler-166	1.37	1.92	2.70	3.80	5.34	7.51	10.56			

Fig. 3.— Observed (black) and predicted (red) distances of exoplanets.

Star	Planet distances [AU]							
Kepler-169	2.15	3.40	4.12	5.80	10.68	19.67		
Kepler-171	2.50	5.21	6.82	8.94	11.72			
Kepler-172	2.06	3.27	6.03	11.11				
Kepler-174	5.76	7.54	9.88	12.95	16.97	22.24	29.14	38.18
Kepler-176	3.00	5.53	8.77	13.93				
Kepler-178	4.58	7.27	9.52	12.48	16.35	21.42		
Kepler-18	2.38	3.78	6.00					
Kepler-184	4.69	7.45	9.76					
Kepler-186	2.35	3.73	5.92	8.32	10.91	14.29	18.72	24.54
Kepler-191	3.34	4.69	6.59					
Kepler-192	3.56	4.66	7.40					
Kepler-194	1.67	2.65	4.20	6.67	13.87			
Kepler-197	3.02	4.80	6.29	8.84				
Kepler-198	1.21	1.70	2.38	3.35	4.71	6.62	13.78	
Kepler-20	2.44	3.43	4.82	6.78	9.53	13.39	18.83	
Kepler-203	2.20	3.09	4.90					
Kepler-206	4.01	5.64	7.92					
Kepler-207	1.33	2.11	3.35					
Kepler-208	2.67	3.76	4.93	6.45				
Kepler-215	4.69	6.14	9.75	15.48				
Kepler-217	2.49	3.02	4.24					
Kepler-218	2.40	3.15	4.13	5.41	7.08	9.28	12.17	25.30
Kepler-219	2.77	3.62	4.75	6.22	8.15	12.94		
Kepler-220	2.61	4.15	5.44	7.12	9.34	13.12		
Kepler-221	2.07	3.29	4.62	6.49				
Kepler-222	2.48	4.57	9.50					
Kepler-223	3.79	4.60	6.02	7.30				
Kepler-224	2.05	3.25	5.16	7.25				
Kepler-226	2.52	3.05	4.00					
Kepler-228	1.88	2.64	4.86					
Kepler-229	3.45	6.36	11.72					
Kepler-23	3.66	4.80	6.29					
Kepler-235	2.15	3.96	7.30	13.44				
Kepler-238	1.65	3.43	5.44					
Kepler-24	2.60	5.41	7.09					
Kepler-244	2.55	4.70	7.45					
Kepler-245	2.07	3.81	7.01	11.13				
Kepler-247	2.21	4.61	7.31					
Kepler-249	2.33	3.70	5.87					
Kepler-250	2.61	3.67	6.77					
Kepler-251	2.95	3.86	5.06	6.63	9.33	12.22	16.01	20.98
Kepler-253	2.55	4.70	6.60					
Kepler-254	3.33	5.29	6.94					
Kepler-255	1.08	1.41	1.85	2.42	3.17	4.46		
Kepler-256	1.45	2.30	3.23	4.54				
Kepler-257	1.76	3.66	4.80	6.28	8.23			
Kepler-26	2.23	3.54	5.62	6.81	12.54			
Kepler-265	3.64	6.71	12.35	16.18				
Kepler-267	2.28	3.62	5.75	9.13				
Kepler-271	2.76	3.20	3.88					
Kepler-272	2.12	3.37	4.73					
Kepler-275	4.93	6.46	10.25					
Kepler-286	1.46	2.31	3.25	4.26	5.58	7.32	9.59	
Kepler-288	3.40	7.07	14.72					
Kepler-289	10.28	16.32	25.91					
Kepler-292	1.82	2.39	3.79	5.33	7.49			
Kepler-295	5.54	7.78	10.20					
Kepler-296	2.32	3.26	4.27	5.60	7.34	10.31	16.37	
Kepler-298	4.98	7.91	10.36	13.58	17.80			
Kepler-299	2.05	3.78	5.99	11.04				
Kepler-30	9.52	15.11	27.84					
Kepler-301	1.92	3.04	5.60					
Kepler-304	1.38	2.19	3.07	4.32				
Kepler-306	2.81	3.69	6.79	12.51				

Star	Planet distances [AU]									
Kepler-31	7.70	12.22	19.40							
Kepler-310	5.81	9.22	14.63	20.57						
Kepler-319	2.61	3.67	5.15	7.25	10.19					
Kepler-32	0.82	1.30	2.06	3.27	4.28	7.89				
Kepler-325	2.67	5.55	11.55							
Kepler-326	1.72	2.74	3.59							
Kepler-327	1.91	3.04	5.59							
Kepler-33	3.04	5.60	7.87	10.31	11.96					
Kepler-331	4.12	6.54	10.39							
Kepler-332	4.01	6.37	10.12							
Kepler-334	3.00	5.52	8.77							
Kepler-336	1.58	2.07	2.71	3.56	4.66	7.39				
Kepler-338	6.01	8.44	11.87							
Kepler-339	2.99	3.62	4.74							
Kepler-341	3.08	4.03	5.28	6.92	9.07	11.88				
Kepler-342	1.43	2.97	6.18	8.69	11.38					
Kepler-351	11.25	14.74	27.16							
Kepler-354	3.12	6.48	8.49							
Kepler-357	3.52	6.48	13.49							
Kepler-359	8.29	15.27	18.50							
Kepler-363	2.43	3.85	5.05							
Kepler-37	5.44	7.64	12.13							
Kepler-372	3.57	7.42	9.73							
Kepler-374	1.57	2.20	2.88							
Kepler-398	2.56	3.60	5.06							
Kepler-399	5.83	9.25	14.69							
Kepler-401	6.03	7.90	10.36	13.57	17.78	23.30	30.53			
Kepler-402	2.53	3.31	4.34	5.04						
Kepler-403	3.61	5.74	9.11	14.46						
Kepler-42	0.61	1.13	1.48							
Kepler-431	3.65	4.23	5.13							
Kepler-444	2.38	2.77	3.35	3.89	4.51					
Kepler-445	2.06	2.89	4.06							
Kepler-446	1.33	2.12	2.98							
Kepler-48	2.82	4.48	6.30	8.86	12.46					
Kepler-49	1.83	3.80	4.98	7.00						
Kepler-52	4.12	6.54	10.39							
Kepler-53	4.51	7.15	11.36							
Kepler-54	4.05	5.31	7.46							
Kepler-55	1.85	2.94	4.66	8.58	11.25					
Kepler-58	4.77	6.25	11.52							
Kepler-60	3.71	4.30	5.21							
Kepler-603	3.52	4.61	6.05	7.92	10.38	13.60	17.82	23.35		
Kepler-62	3.24	5.14	6.74	8.83	11.57	15.17	19.87	26.04	41.34	
Kepler-68	3.13	4.40	6.98	11.08	17.58	27.91	44.30	70.33		
Kepler-758	2.87	4.03	5.28	7.43						
Kepler-770	1.25	2.61	3.67	5.16	7.25					
Kepler-79	5.65	8.97	14.23	18.65						
Kepler-80	1.02	2.12	2.78	3.64	4.41					
Kepler-81	3.33	5.28	7.43							
Kepler-82	1.75	3.22	4.53	6.36	8.95	14.20				
Kepler-83	2.93	4.66	7.39							
Kepler-84	2.68	4.25	5.57	8.84	12.42					
Kepler-85	4.08	5.35	7.01	8.49						
Kepler-89	2.38	4.96	7.87	14.49						
Kepler-9	1.33	1.87	2.63	3.69	5.19	7.30	11.59			
PSR-B1257+12	8.78	16.17	21.19							
TRAPPIST-1	1.29	1.82	2.55	3.35	4.38	5.31	7.47			
WASP-47	2.68	4.25	6.74	10.70	16.99	26.97	42.81	67.96		
mu-Ara	4.19	7.71	14.21	26.18	48.22	76.54	140.99	259.70		
upsilon-And	3.03	5.59	10.29	18.95	34.91	64.31	118.45			